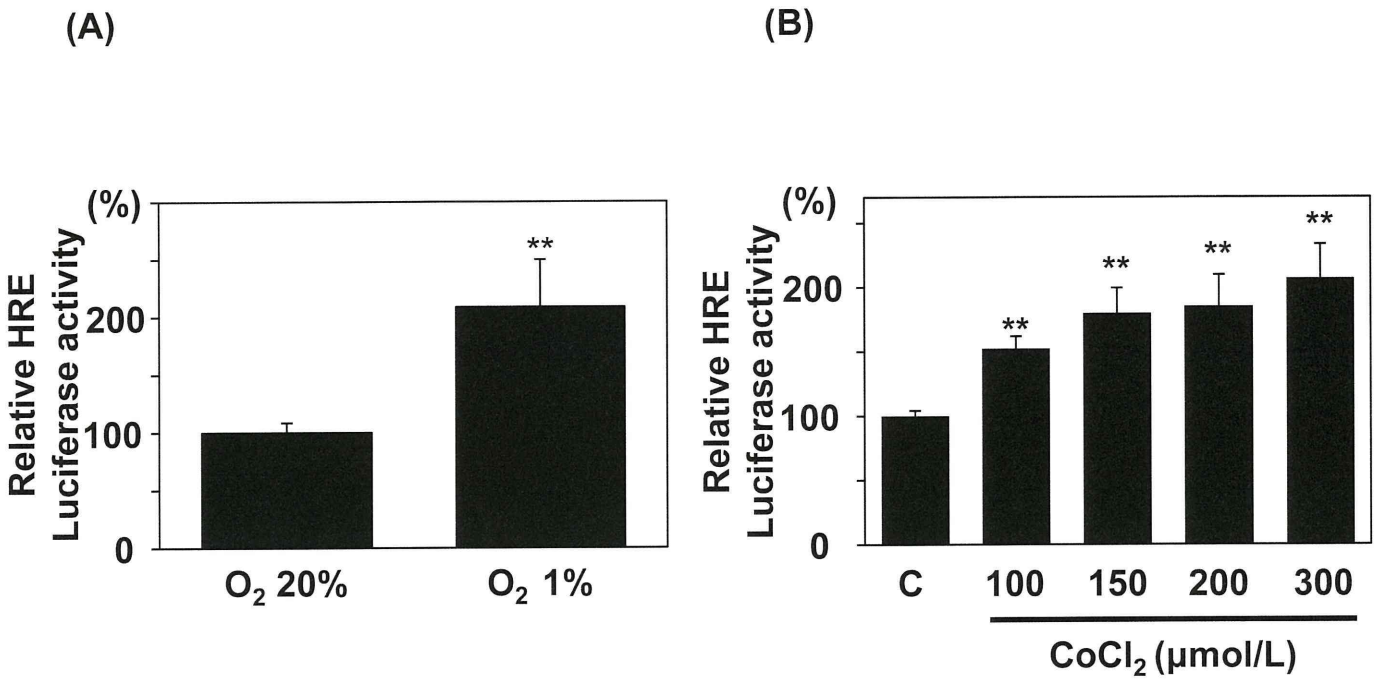

Figure S3. Hypoxia and $CoCl_2$ increased HRE-driven promoter activity.
HRE luciferase DNA construct and LacZ gene were introduced into VSMCs. VSMCs were incubated for 24 hours (A) under hypoxia (O_2 1%) or (B) with varying concentrations of $CoCl_2$ as indicated in the figure. Luciferase activity was normalized by β-galactosidase activity. Relative luciferase activity obtained in VSMC culture at 20% O_2 concentration or control culture (C) was set as 100%. Data are shown as mean±SEM (n=7, n=3, respectively). **P<0.01 vs O_2 20% or C.

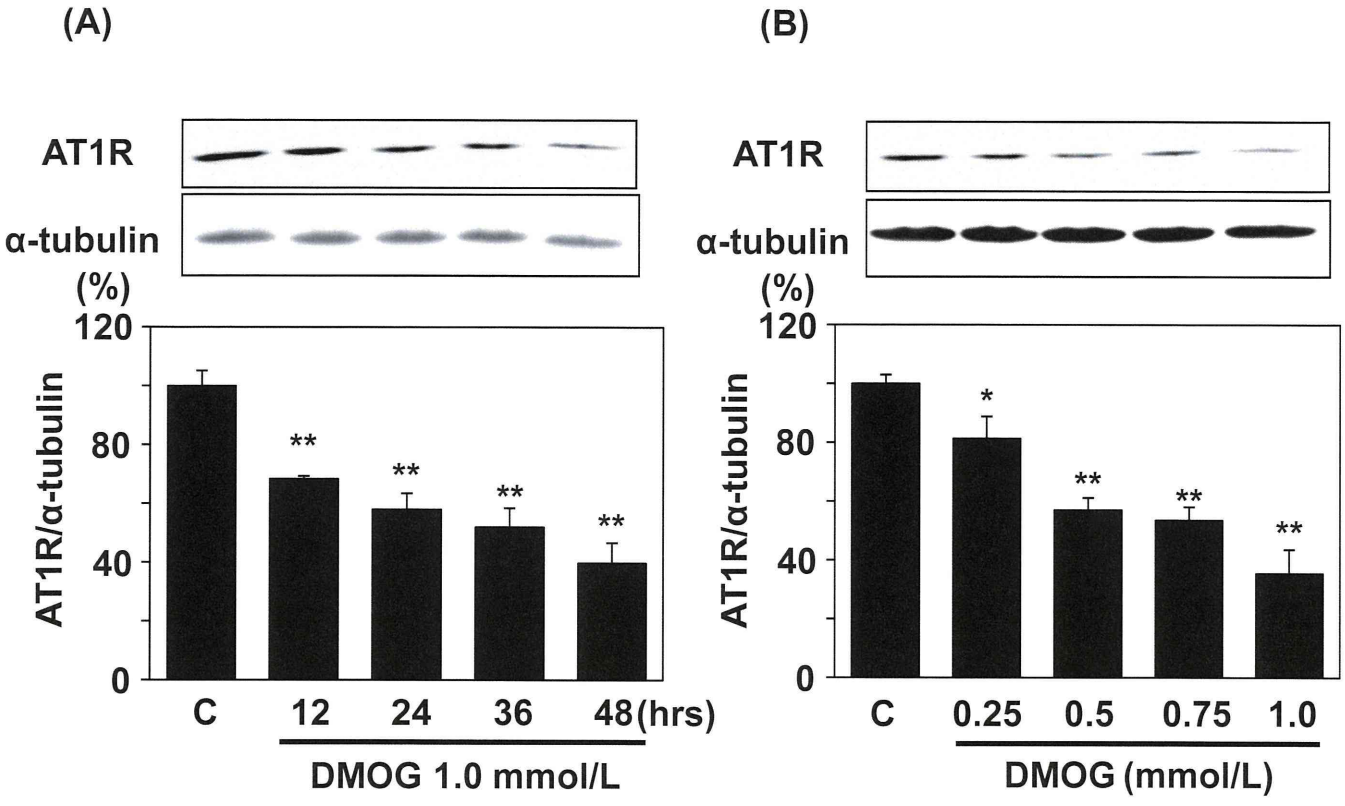

Figure S4. DMOG, another PHD inhibitor, also suppressed AT1R expression.
(A) VSMCs were incubated with DMOG (1.0 mmol/L) for varying periods as indicated in the figure (n=4). (B) VSMCs were incubated with DMOG at varying concentrations as indicated in the figure for 48 hours (n=4). (A), (B) Expression of AT1R and α-tubulin protein was detected by Western blot analysis. The ratio of AT1R to α-tubulin is shown in the bar graph. Values (mean±SEM) are expressed as a percentage of control culture (100%). *P<0.05, **P<0.01 vs control (C).

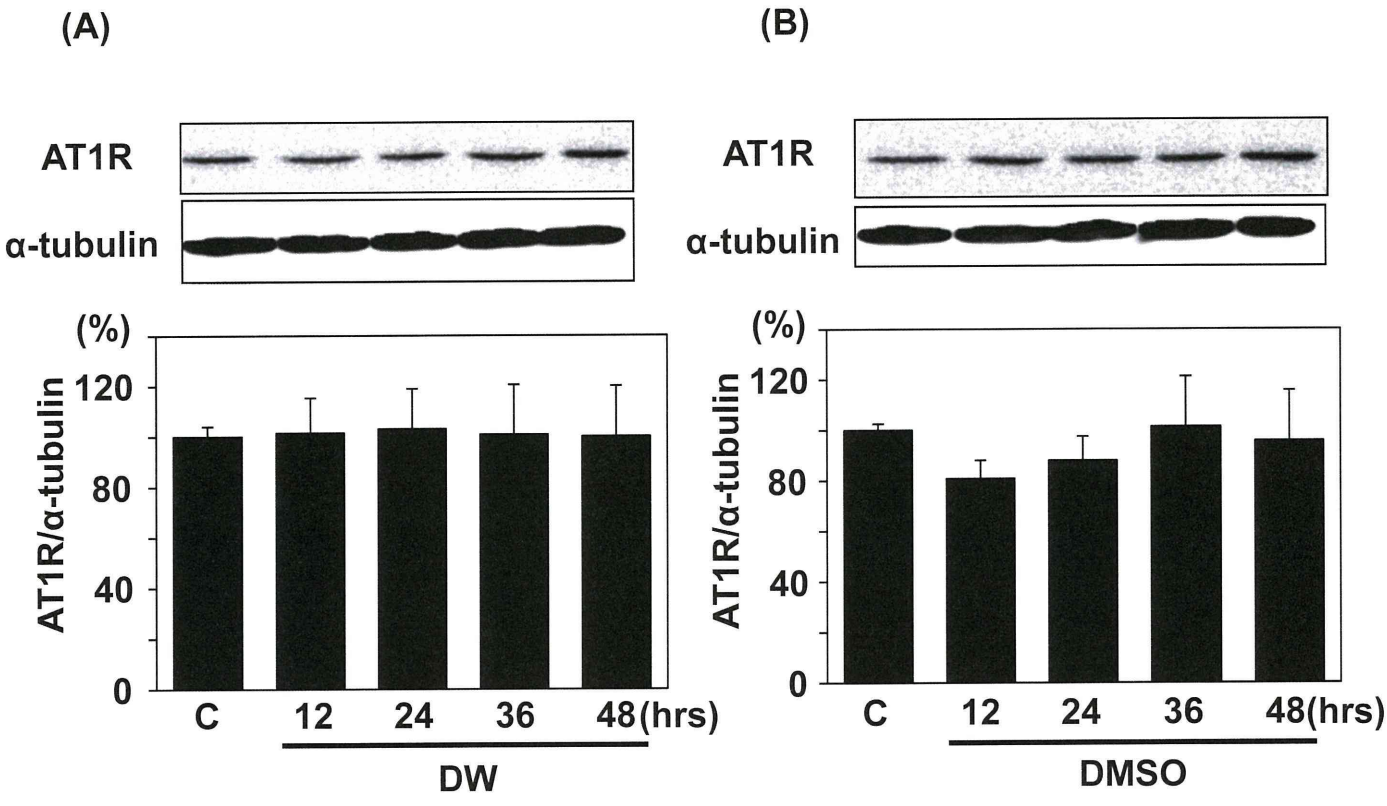

Figure S5. Control vehicle did not affect expression of AT1R protein.
(A) and (B) The same volume of vehicle (distilled water (DW) for $CoCl_2$ and dimethyl sulfoxide (DMSO) for DMOG) used to dissolve the chemical reagents at maximal doses was added to culture medium and VSMCs were incubated for varying periods as indicated in the figure (n=4). Expression of AT1R and α-tubulin protein was detected by Western blot analysis. The ratio of AT1R to α-tubulin is shown in the bar graph. Values (mean±SEM) are expressed as a percentage of control culture (100%).

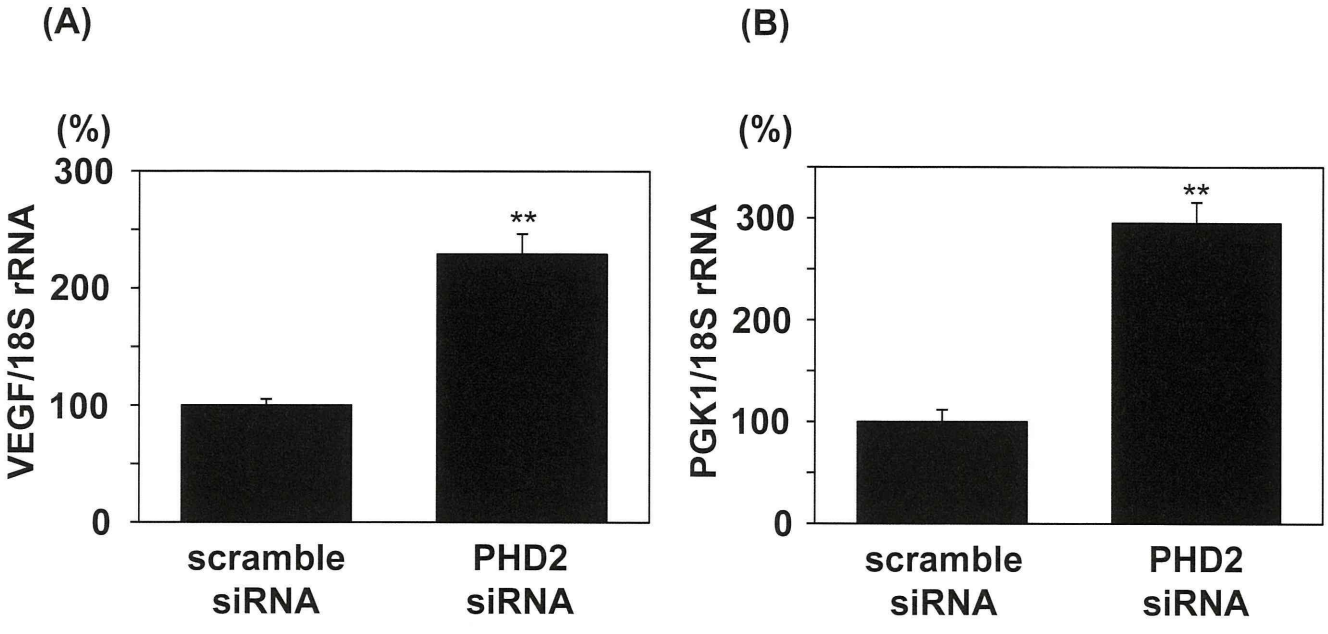

Figure S6. Knockdown of PHD2 mRNA upregulated VEGF and PGK1 mRNA expression. VSMCs were transfected with scramble siRNA or PHD2-specific siRNA. After 72 hours, the expression of VEGF (A) and PGK1 (B) was evaluated by Real-time Quantitative RT-PCR. The ratio of VEGF or PGK1 mRNA to 18S rRNA is shown in the bar graph. (n=3) Values (mean±SEM) are expressed as a percentage of scramble siRNA (100%). **P<0.01 vs scramble siRNA.

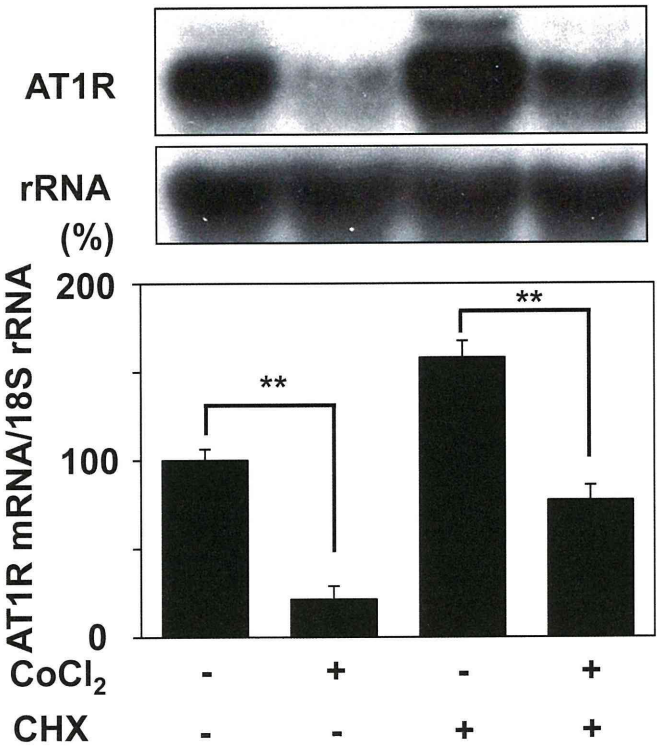

Figure S7. Effect of CHX on $CoCl_2$-Induced AT1R mRNA downregulation.
VSMCs were preincubated with or without CHX (10 μg/mL) for 30 minutes and then incubated in the presence or absence of $CoCl_2$ (200 μmol/L) for 24 hours. Expression of AT1R mRNA and 18S rRNA was determined by Northern blot analysis as described in the legend to Figure 1. Values (mean±SEM) are expressed as a percentage of control culture (100%) n=4. **P<0.01.

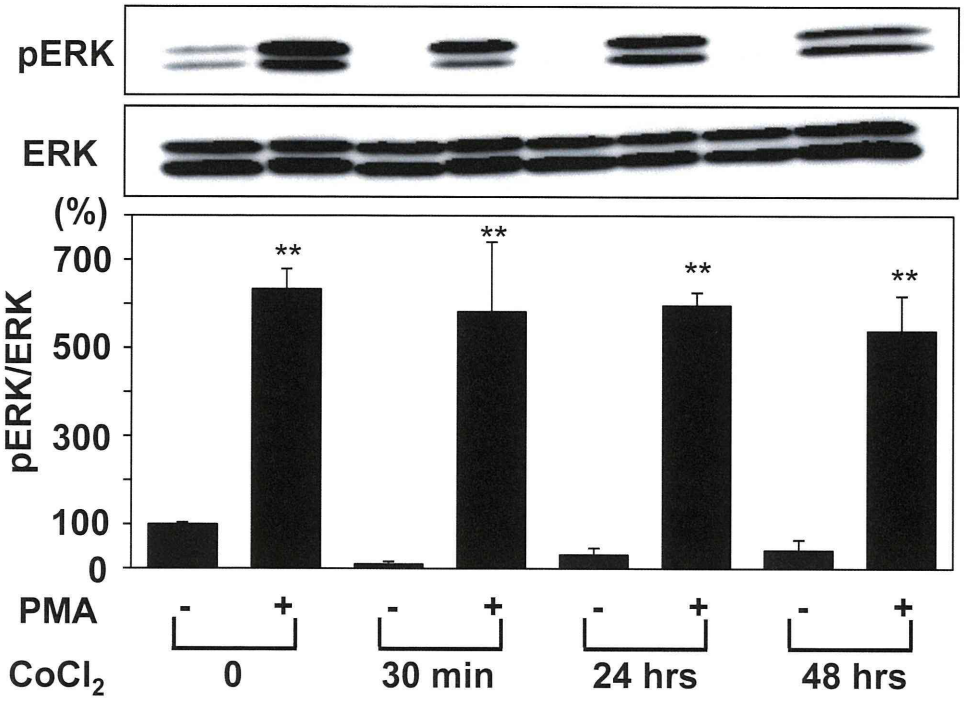

Figure S8. PMA-induced ERK phosphorylation was not affected by $CoCl_2$.
VSMCs were pretreated with $CoCl_2$ (200 μmol/L) for 30 minutes, 24 hours, and 48 hours, and then stimulated with or without PMA (100 nmol/L) for 5 minutes. pERK and ERK protein were detected by Western blot analysis. The ratio of pERK to ERK is shown in the bar graph. Values (mean±SEM) are expressed as a percentage of control culture (100%) n=4. **P<0.01 vs PMA (-) at each time points.

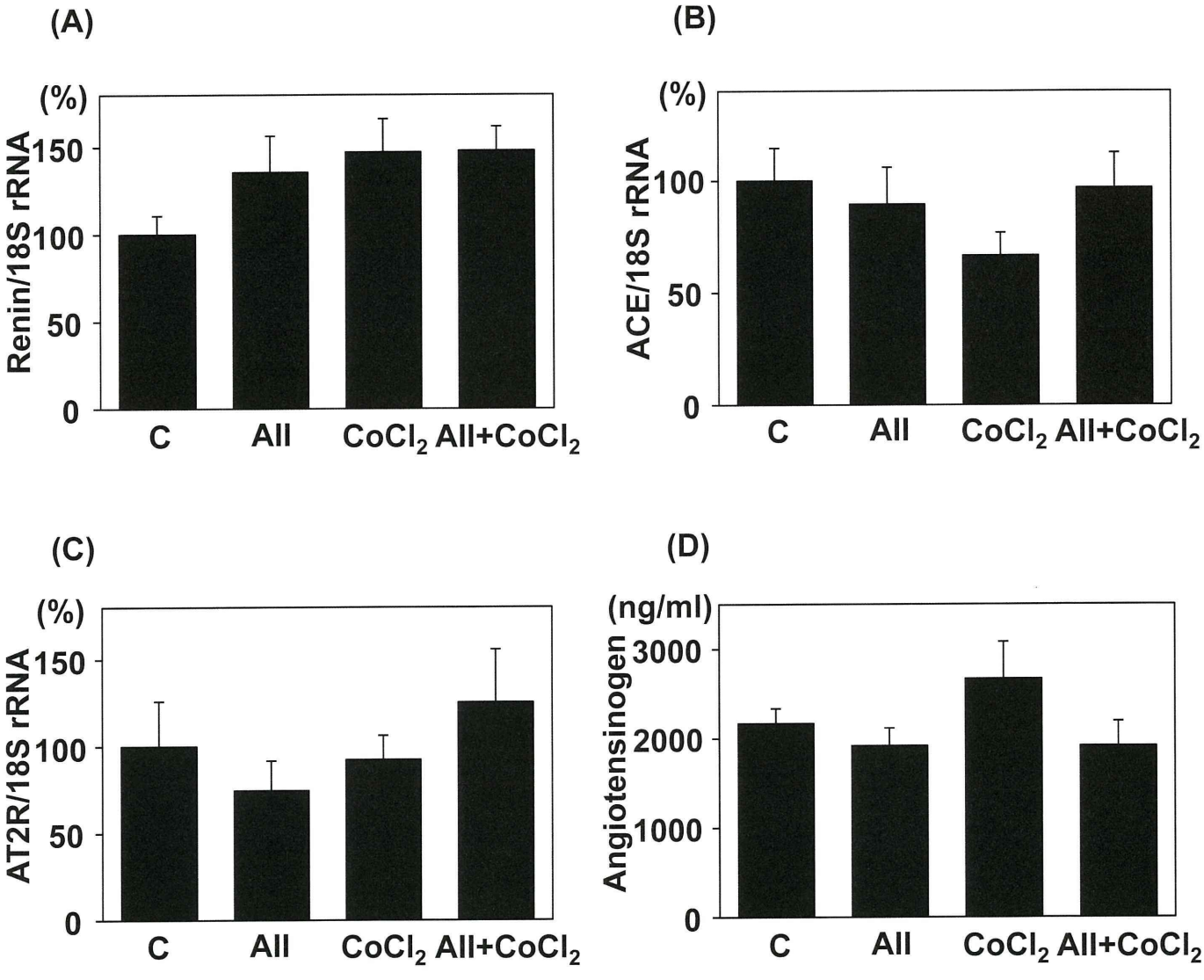

Figure S9. Renin, ACE, and AT2R mRNA of the mice aorta and serum Angiotensinogen. (A), (B) and (C) Expression of Renin mRNA from kidneys and ACE and AT2R mRNA from aortas of mice in each group of the animal experiment was examined by real time quantitative RT PCR. The ratio of Renin, ACE, and AT2R mRNA to 18S is shown in the bar graph. (D) Serum concentration of Angiotensinogen in each group of the animal experiment was examined by ELISA. Values (mean±SEM) are expressed as a percentage of control mice (100%).

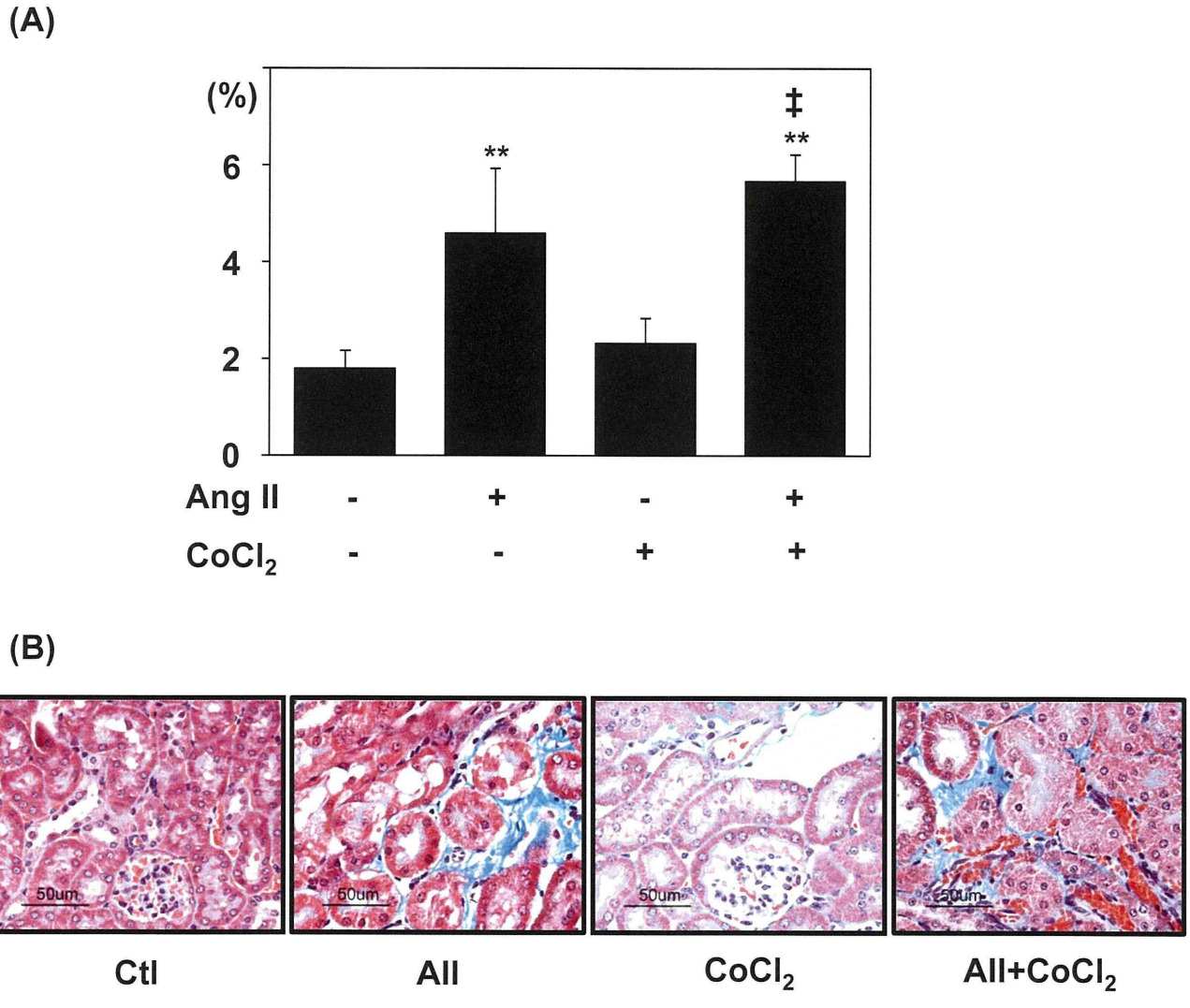

Figure S10. $CoCl_2$ did not affect AII-induced interstitial fibrosis of the kidney in mice. Interstitial fibrosis of the kidneys was examined. Ang II significantly increased interstitial fibrosis of the kidneys. $CoCl_2$ did not inhibit the Ang II-induced interstitial fibrosis of the kidneys. (n=5–6, each group). **P<0.01 vs Ang II (-) and $CoCl_2$ (-). ‡P<0.01 vs Ang II (-) and $CoCl_2$ (+). (B) Representative microphotographs of Masson's Trichrome-stained mice kidneys from each group are shown. (n=5–6, each group).

Brain AT_1 Receptor Activates the Sympathetic Nervous System Through Toll-like Receptor 4 in Mice With Heart Failure

Kiyohiro Ogawa, MD, Yoshitaka Hirooka, MD, PhD,† Takuya Kishi, MD, PhD,‡ and Kenji Sunagawa, MD, PhD**

Abstract: The activation of angiotensin II type 1 receptor (AT_1R) in the brain plays a pivotal role in enhanced sympathetic drive in heart failure (HF). Activation of the AT_1R in the brain produces oxidative stress and inflammation. Toll-like receptor 4 (TLR4) signaling in the brain induces the inflammatory cascade. We hypothesized that sympathoexcitation is mediated by the AT_1R-activated TLR4 in the brainstem in HF. As a model of HF, the left coronary artery was ligated to induce a large myocardial infarction and subsequent chronic heart failure (CHF) in Institute of Cancer Research mice. On day 10 after the surgery, we started intracerebroventricular infusion of losartan (CHF-Los) or vehicle (CHF-Veh) via osmotic minipumps for 14 days. Expression level of the TLR4 in the brainstem was significantly higher in HF mice than in sham mice and significantly lower in CHF-Los mice than in CHF-Veh mice. Urinary norepinephrine excretion was significantly higher in HF mice than in sham mice and was significantly lower in CHF-Los than in CHF-Veh. Chronic intracerebroventricular infusion of angiotensin II increased the expression level of the second messenger of the TLR4. These results suggest that activation of the TLR4 via AT_1R in the brainstem contributes to the sympathoexcitation probably due to the inflammation in the brain of the myocardial infarction–induced HF.

Key Words: heart failure, toll-like receptor, angiotensin II, brain inflammation

(*J Cardiovasc Pharmacol*™ 2011;58:543–549)

INTRODUCTION

Heart failure (HF) is characterized by the activation of sympathetic nervous system (SNS),[1,2] and the activation of the SNS contributes to the increased mortality and/or left ventricular (LV) dysfunction.[2–5] Previous studies have shown that the activation of the renin–angiotensin system (RAS) in the brain, in particular, the cardiovascular center in the brainstem, evokes the activation of the SNS in the HF and that the increase in oxidative stress is responsible for the brain angiotensin II type 1 receptor (AT_1R)–induced activation of the SNS in the HF.[6–12] However, the downstream of the AT_1R and oxidative stress in the brain have not been fully determined.

Recent studies have suggested that the inflammation cascade in the brain is one of the important pathways in the activation of the SNS in the cardiovascular diseases.[13–17] Central inflammation activates the SNS via nicotinamide adenine dinucleotide phosphate (NAD(P)H) oxidase-dependent mitogen-activated protein kinase (MAPK) signaling.[17] In the brain, after the myocardial infarction (MI), proinflammatory cytokines stimulates the activity of the SNS by inducing cyclooxygenase 2 activity and prostaglandin E_2 production in perivascular macrophages of the blood–brain barrier.[14] Furthermore, the RAS in the brain is a major mechanism for sympathetic hyperactivity, LV remodeling, and LV dysfunction after the MI.[11] Previously, we demonstrated that the AT_1R and NAD(P)H oxidase—induced apoptotic pathway through the MAPK in the cardiovascular center of the brainstem contributes to the activation of the SNS.[18] These results suggested that the RAS and inflammatory pathway in the brainstem cause the sympathoexcitation in the MI-induced HF. In the inflammatory cascade, toll-like receptors (TLRs) signaling plays an important role in immune response to pathogens.[19] After the stimulation with an appropriate ligand, the TLRs relay a signal via myeloid differentiation primary response protein 88 (MyD88), a common signal adaptor molecule, and trigger the downstream stimulation of the nuclear factor-κB (NF-κB) and the induction of genes that encode proinflammatory cytokines.[19] The inflammatory response is usually associated with the activation of innate immunity, specifically with the TLRs.[19] Among the TLRs, the role of the TLR4 in the brain damage of stroke, neurodegenerative diseases, and alcohol ingestion has been suggested.[20–23] Furthermore, several previous reports have suggested that the locally produced angiotensin II causes the inflammation via TLR4 pathway.[24,25] However, the role of the TLR4 in the brain in the regulation of the SNS has not been determined.

Therefore, we hypothesized that the AT_1R in the brain may activate the SNS through in part the inflammation mediated by the TLR4 in the MI-induced HF, and the aim of the present study was to determine whether the inhibition of the

Received for publication May 31, 2011; accepted July 18, 2011.

From the Departments of *Cardiovascular Medicine; and †Advanced Cardiovascular Regulation and Therapeutics; and ‡Advanced Therapeutics for Cardiovascular Diseases, Kyushu University Graduate School of Medical Sciences, Fukuoka, Japan.

Supported by Grants-in-Aid for Scientific Research from the Japan Society for the Promotion of Science (B193290231, 22790709, and S23220013) and, in part, by a Kimura Memorial Foundation Research Grant.

The authors report no conflicts of interest.

Reprints: Yoshitaka Hirooka, MD, PhD, FAHA, Department of Advanced Cardiovascular Regulation and Therapeutics, Kyushu University Graduate School of Medical Sciences, 3-1-1 Maidashi, Higashi-ku, Fukuoka 812-8582, Japan (e-mail hyoshi@cardiol.med.kyushu-u.ac.jp).

activation of SNS via blockade of the AT_1R in the brain is through the TLR4 or not. For this purpose, we performed the chronic intracerebroventricular (ICV) infusion of the AT_1R blocker, losartan, to the mice with the MI-induced HF and examined the effects of the AT_1R blocker on the activation of the SNS and LV remodeling with the expression levels of the TLR4, MyD88, and NF-κB in the brainstem.

MATERIALS AND METHODS

Animal Model and General Procedures

This study was reviewed and approved by the committee on ethics of Animal Experiments, Kyushu University Graduate School of Medical Sciences, and conducted according to the Guidelines for Animal Experiments of Kyushu University. Male Institute of Cancer Research (ICR) mice (7–8 weeks old) were obtained from SLC Japan (Hamamatsu, Japan). Mice were fed a standard diet, and each strain was divided into 4 groups, sham-operated (Sham), chronic heart failure (CHF), CHF treated with vehicle (CHF-Veh), and CHF treated with losartan (CHF-Los).

Induction of CHF

We experimentally induced MI and subsequent CHF in ICR mice. Under anesthesia with pentobarbital and under mechanical ventilation, the thorax was opened at left intercostals space, and the left coronary artery (LCA) was ligated at 2 to 3 mm from its origin with 8-0 silk. Sham control mice underwent the same surgical procedure without ligation. After the experimental protocols, mice were euthanized with pentobarbital. The brain was removed and immediately frozen on dry ice. Moreover, the lung and heart were removed immediately and weighed.

Chronic ICV Infusion of Losartan or Vehicle to the CHF Mice

At day 10 after the interventions (LCA occlusion and sham operation), mice were instrumented with ICV cannula for chronic infusion of the losartan (10 μg/h; Sigma-Aldrich, St Louis, MO)[26] or artificial cerebrospinal fluid (aCSF) into the lateral ventricles in the CHF-Los and CHF-Veh groups. Under light anesthesia of pentobarbital, mice were placed in a stereotaxic apparatus. The head of the mice were aligned so the lambda–bregma plane was horizontal, and a hole was made 0.4 mm posterior and 1.0 mm lateral to the bregma. The 30-gauge L-shaped cannula was inserted 0 mm below the skull surface and fixed with adhesive. The ICV cannula was connected, via a PE50 catheter, to a mini-osmotic pump implanted subcutaneously (Alzet; model 1002).

Echocardiographic Analysis

Echocardiographic studies were performed under light anesthesia of pentobarbital. An echocardiography system with dynamically focused 7.5-MHz linear array transducer was used. Two-dimensional parasternal short-axis view of the LV was obtained, and LV dimensions were measured.

Evaluation of the Activity of the SNS

As described previously, we measured the 24-hour urinary norepinephrine excretion at 4 weeks after the ligation of the LCA as a parameter of the activity of the SNS.[16,18,27–29]

Expression Levels of the TLR4 and MyD88 in the Brainstem

Western blot analysis was performed to determine the expression levels of the TLR4 (1:250; Santa Cruz Biotechnology, Santa Cruz, CA) and MyD88 (1:500; Cell Signaling Technology) of the brainstem as described previously.[16,18,27–29]

Electrophoretic Mobility Shift Assay

The NF-κB binding activity in the brainstem was measured by electrophoretic mobility shift assay. The brainstem tissue (30–40 mg) was suspended in hypotonic Tris buffer [400 μL; 10 mM Tris–HCl (pH 7.8), 5 mM $MgCl_2$, 10 mM KCl, 0.2 mM EDTA, 0.5 mM dithiothretiol (DTT), 0.3 M sucrose, and 1 mM phenylmethylsulfonyl fluoride] and was homogenated. After the solution had been kept on ice for 15 minutes, 10% Nonidet P40 (20 μL) was added followed by centrifugation at 8000*g* for 1 minute. The pellet was suspended in high-salt Tris buffer [100 μL; 20 mM Tris–HCl (pH 7.8), 5 mM $MgCl_2$, 0.2 mM EDTA, 0.5 mM DTT, 1 mM phenylmethylsulfonyl fluoride, and 320 mM KCl] on ice for 15 minutes. After centrifugation at 13500*g* for 15 minutes, the supernatant liquid, containing nuclear protein, was collected. Probe for NF-κB was synthesized as double-stranded oligomers: 5′-AGTTGAGGGGACTTTCCCAGGC-3′. This probe was end-labeled with [γ-^{32}P]-ATP by the activity of T4 polynucleotide kinase (Promega, Madison, WI). For this analysis, 2 μg of nuclear extract was preincubated for 10 minutes with 2 μg of poly-(dl-dC) and bovine serum albumin in 4 μL of binding buffer [100 mM Tris–HCl (pH 7.5), 10 mM EDTA, 40% glycerol, 1 M NaCl, and 100 mM DTT]. The probe was then added to the reaction mixture, which was incubated for 20 minutes. Subsequently, each sample was subjected to 5% polyacrylamide gel electrophoresis in buffer. Autoradiography was performed on the dried gel.

Chronic ICV Infusion of Exogenous Angiotensin II or Vehicle to the Normal Control Mice

To determine whether the brain AT_1R stimulation exogenously activate TLR4 in the brain, thereby increasing the central sympathetic outflow in normal control mice, we performed the chronic ICV infusion of exogenous angiotensin II (Ang II group) or aCSF (Veh group) to the normal male ICR mice without MI. Mice were instrumented with ICV cannula for the chronic infusion of angiotensin II (600 $ng \cdot kg^{-1} \cdot min^{-1}$; Sigma-Aldrich) or aCSF for 14 days. The dose of angiotensin II was determined according to the previous report in which the ICV of angiotensin II causes the sympathoexcitation in mice.[30]

Statistical Analysis

All values are expressed as mean ± standard error of the mean. Comparisons between any 2 mean values were

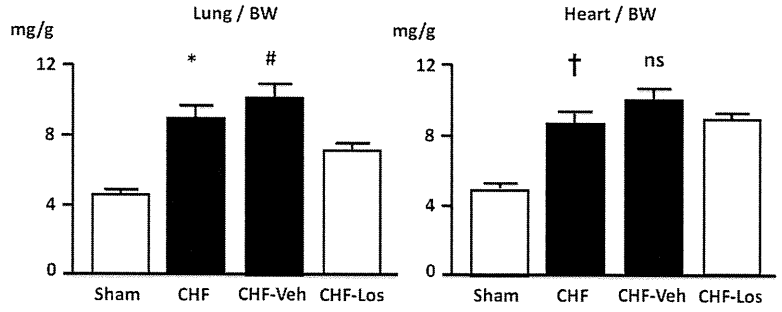

FIGURE 1. Organ weight of post-MI and sham-operated mice. Left, lung weight/body weight (BW) (*$P < 0.05$ vs. Sham group, #$P < 0.05$ vs. CHF-Los group, n = 6 for each group). Right, heart weight/BW (†$P < 0.05$ vs. Sham group, n = 6 for each group). Data are shown as mean ± standard error of the mean.

performed using Bonferroni correction for multiple comparisons. Analysis of variance was used to compare all the parameters in the CHF, Sham, CHF-Veh, and CHF-Los groups. Differences were considered to be statistically significant at a P value of <0.05.

RESULTS

Measurement of Body Weight, Organ Weight, and Echocardiographic Data in CHF Mice

Mice developed CHF within 4 weeks after the MI. The weights of lung and heart were significantly higher in the CHF group than in the Sham group (Fig. 1). However, lung weights were significantly lower in the CHF-Los group than in the CHF-Veh group (Fig. 1). The percent fractional shortening was significantly lower, and LV diastolic diameter and LV systolic diameter were significantly higher in the CHF group than in the Sham group (Table 1). However, %FS was significantly higher, and LV diastolic diameter and LV systolic diameter were significantly lower in the CHF-Los group than in the CHF-Veh group (Table 1).

Urinary Norepinephrine Excretion as an Indicator of the Activation of the SNS

Urinary norepinephrine excretion was significantly higher in the CHF group than in the Sham group (Fig. 2). However, urinary norepinephrine excretion was significantly lower in the CHF-Los group than in the CHF-Veh group (Fig. 2).

TABLE 1. Echocardiographic Measurements

	LVDd (mm)	LVDs (mm)	%FS	Anterior Wall (mm)	Posterior Wall (mm)
Sham	3.43 ± 0.19	1.58 ± 0.16	53.7 ± 3.2	0.98 ± 0.07	1.02 ± 0.06
CHF	5.63 ± 0.12*	4.67 ± 0.11*	16.3 ± 0.6*	0.65 ± 0.04*	1.30 ± 0.04*
CHF-Veh	5.85 ± 0.07#	4.82 ± 0.06#	17.7 ± 0.7#	0.55 ± 0.07	1.35 ± 0.03
CHF-Los	5.43 ± 0.06	3.80 ± 0.07	30.8 ± 1.2	0.63 ± 0.05	1.32 ± 0.05

Data are shown as mean ± standard error of the mean.
*$P < 0.05$ versus Sham group.
#$P < 0.05$ versus CHF-Los group, n = 6 for each group.
CHF, chronic heart failure induced by ligation of left coronary artery; Los, losartan; LVDd, left ventricular diastolic diameter; LVDs, left ventricular systolic diameter; Sham, sham-operated mice; Veh, vehicle (aCSF); %FS, percent fractional shortening.

Expression Levels of the TLR4 and MyD88 in the Brainstem

The expression levels of the TLR4 and MyD88 in the brainstem were significantly higher in the CHF group than in the Sham group and significantly lower in the CHF-Los group than in the CHF-Veh group (Fig. 3).

NF-κB Binding Activity

Binding activity of the transcription factor NF-κB was significantly higher in the CHF group than in the Sham group and significantly lower in the CHF-Los group than in the CHF-Veh group (Fig. 4).

Chronic ICV Infusion of Exogenous Angiotensin II to the Normal Control Mice

Chronic ICV infusion of exogenous angiotensin II caused the sympathoexcitation (Fig. 5) as described in the previous study.[30] The expression level of the TLR4 in the brainstem was not different between the Ang II group and the Veh group (Fig. 6). However, the expression level of the MyD88 in the brainstem was significantly higher in the Ang II group than in the Veh group (Fig. 6).

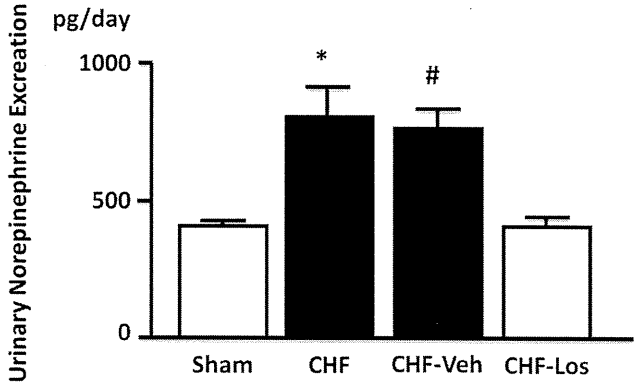

FIGURE 2. Twenty-four–hour urinary norepinephrine excretion as an indicator of activity of the SNS (*$P < 0.05$ vs. Sham group; #$P < 0.05$ vs. CHF-Los group, n = 4 for each group).

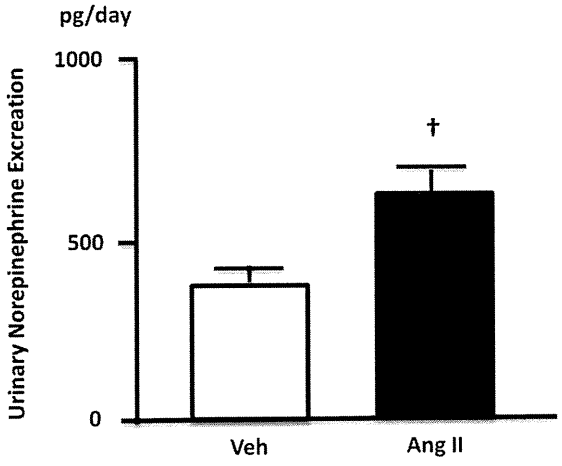

FIGURE 3. A, Western blots demonstrating the expression levels of the TLR4 and MyD88 in the brainstem in CHF group and Sham group (*$P < 0.05$ vs. Sham group, n = 5, for each group). B, Western blots demonstrating the expression levels of the TLR4 and MyD88 in the brainstem in the CHF-Veh group and CHF-Los group (#$P < 0.05$ vs. CHF-Los group, n = 5, for each group).

DISCUSSION

The present study demonstrated that the expression levels of the TLR4 and MyD88, the second messenger of the TLR4, in the brainstem are enhanced in mice with the MI-induced HF and that the ICV infusion of the AT_1R blocker reduces the enhanced activity of the SNS associated with the inhibition of the expression levels of the TLR4, MyD88, and NF-κB in the brainstem. Furthermore, chronic exogenous infusion of angiotensin II into the brain activates the SNS with the increase in the expression level of the MyD88. Our findings provide a novel insight, suggesting that the AT_1R in the brainstem activates the SNS through in part the inflammation mediated by the TLR4 and MyD88 in mice with the MI-induced HF (Fig. 7).

Previous studies have suggested that the central inflammation activates the SNS[17] and that the RAS in the brain evokes the sympathetic hyperactivity, LV remodeling, and LV dysfunction in the MI-induced HF.[11,14] These findings suggest that the RAS and inflammation have a close relationship in the brain of the MI-induced HF mice. It has been shown that angiotensin II activates the TLR4[24,25] and that the AT_1R blocker inhibits the TLR4 in the mesangial and smooth muscle cells.[31–34] In the present study, we demonstrated that the blockade of AT_1R in the brainstem decreases the expression levels of the NF-κB, TLR4, and MyD88 in the MI-induced HF and that the ICV infusion of angiotensin II increases the expression levels of the NF-κB and MyD88. Exogenous angiotensin II infusion does not increase the expression level of the TLR4. However, the expression levels of the MyD88, the downstream of the TLR4, were increased by the exogenous infusion of angiotensin II. These findings suggest that the AT_1R stimulation in the brain by angiotensin II infusion elicits the TLR4–MyD88 activation because the increase in the expression level of the MyD88 strongly indicates the activation of the AT_1R and TLR4. We cannot exclude the possibility that other factors might also contribute to the activation of the TLR4–MyD88 pathway in the MI-induced HF. Another possibility is that exogenous angiotensin II infusion into the brain for 2 weeks might be insufficient for increasing the expression level of the TLR4. However, our findings support the concept that the AT_1R-induced

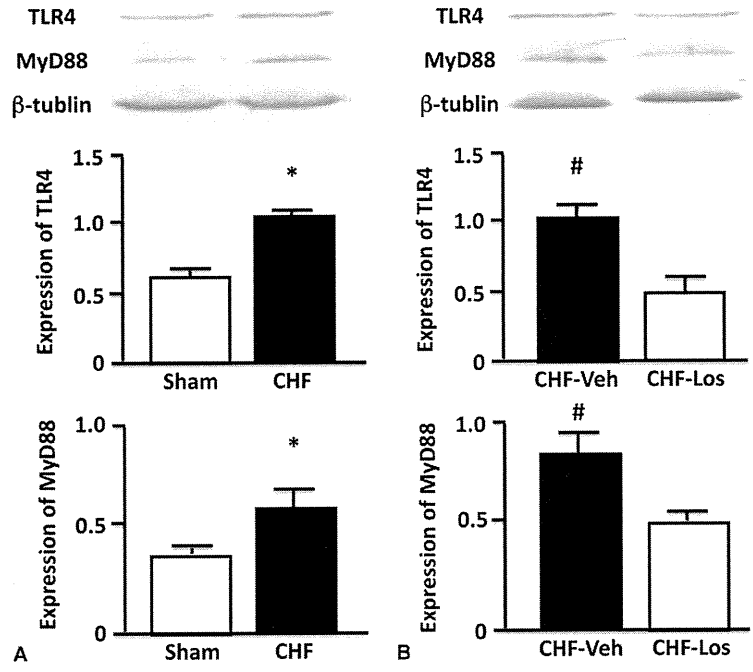

FIGURE 4. Electrophoretic mobility shift assay demonstrating the NF-κB binding activity in the brainstem in each group.

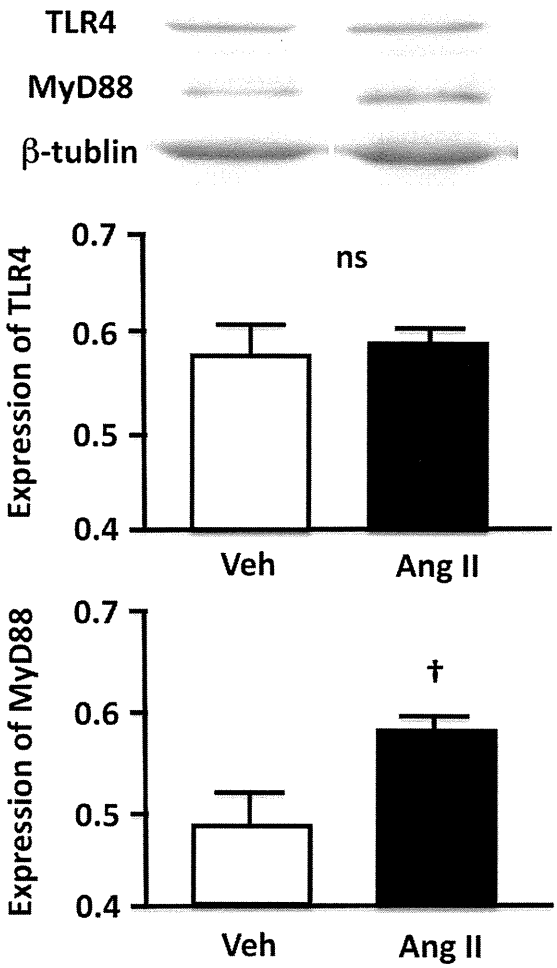

FIGURE 5. Twenty-four–hour urinary norepinephrine excretion as an indicator of activity of the SNS in the Ang II and Veh groups (†$P < 0.05$ vs. Veh group, n = 4 for each group). Data are shown as mean ± standard error of the mean.

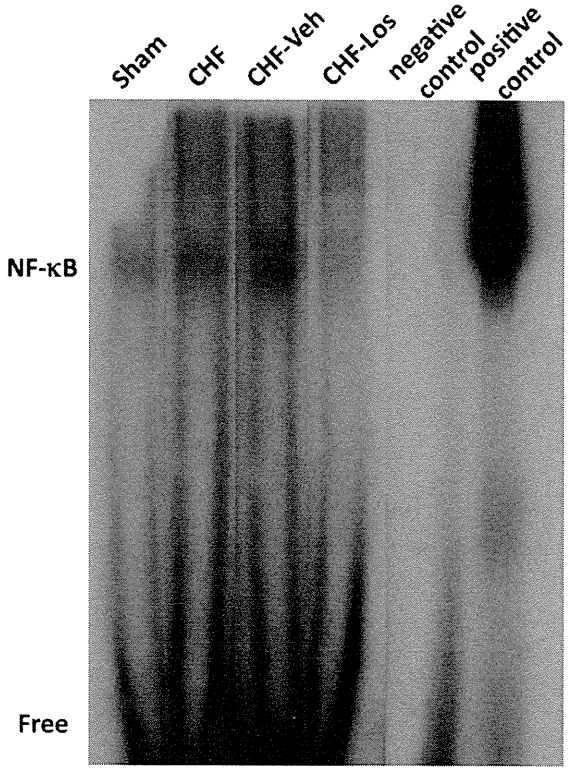

FIGURE 6. Western blots demonstrating the expression levels of the TLR and MyD88 in the brainstem in the Ang II group and Veh group (†$P < 0.05$ vs. Veh group, n = 4, for each group). Data are expressed as the ratio to the expression of the β-tubulin. Data are shown as mean ± standard error of the mean.

inflammation mediated by the TLR4 and MyD88 in the brainstem is in part involved in the sympathetic hyperactivity and LV remodeling in the MI-induced HF and might be a new target of the treatment of the MI-induced HF (Fig. 7).

Accumulating evidence indicates that the RAS in the brain contributes to the activation of the SNS via reactive oxygen species (ROS).[7,9,11,12,18,29,30,35] Previous studies have suggested that the RAS activates the SNS via brain ROS in the MI-induced HF.[7,9,11,12] Interestingly, we have demonstrated that inducible NOS, a key enzyme of the inflammation, in the brain activates the SNS[13,16] and that the AT_1R in the brain activates the SNS through the neural apoptosis in hypertensive model rats.[18] Based on these findings, we consider that the inflammatory cascade via ROS induced by the AT_1R in the brain might activate the SNS. In fact, we found that the enhanced expression level of the NF-κB was decreased after the blockade of the AT_1R in the brain of the MI-induced HF mice. Although we did not measure the oxidative stress in the brainstem of the MI-induced HF mice and did not determine the relationship between ROS and TLR4 in the present study, previous studies have indicated that the AT_1R in the brainstem activates the SNS via ROS in the MI-induced HF.[7,9,11,12] Therefore, it is possible that the inflammation mediated by the TLR4 and MyD88 in the brain might be one of the key mediators in the sympathoexcitation via ROS in the brain of the MI-induced HF mice.

The important finding of the present study was that central inhibition of the AT_1R in the brain reduced the expression levels of the TRL4 and MyD88 and the activity of the SNS, thereby improving the remodeling process in the MI-induced HF. A previous report suggests that the pharmacological systemic inhibition of the MyD88 protected against the LV dilatation and hypertrophy, and this protection occurred despite no measurable reduction in infarct size.[36] In the present study, we infused the AT_1R blocker or angiotensin II into the brain by the ICV infusion and did not determine the exact site in which these agents affect the brain. The dose of losartan and angiotensin II used in the present study was insufficient to act peripherally. There are several important autonomic nuclei in the central nervous system, including the brainstem nuclei and the hypothalamus,[37,38] and the AT_1R in the brain distributes richly in those nuclei.[39–41] Furthermore, the AT_1Rs in those nuclei are upregulated, associated with the sympathoexcitation in the MI-induced HF.[7,9,11,12] Therefore, it is possible

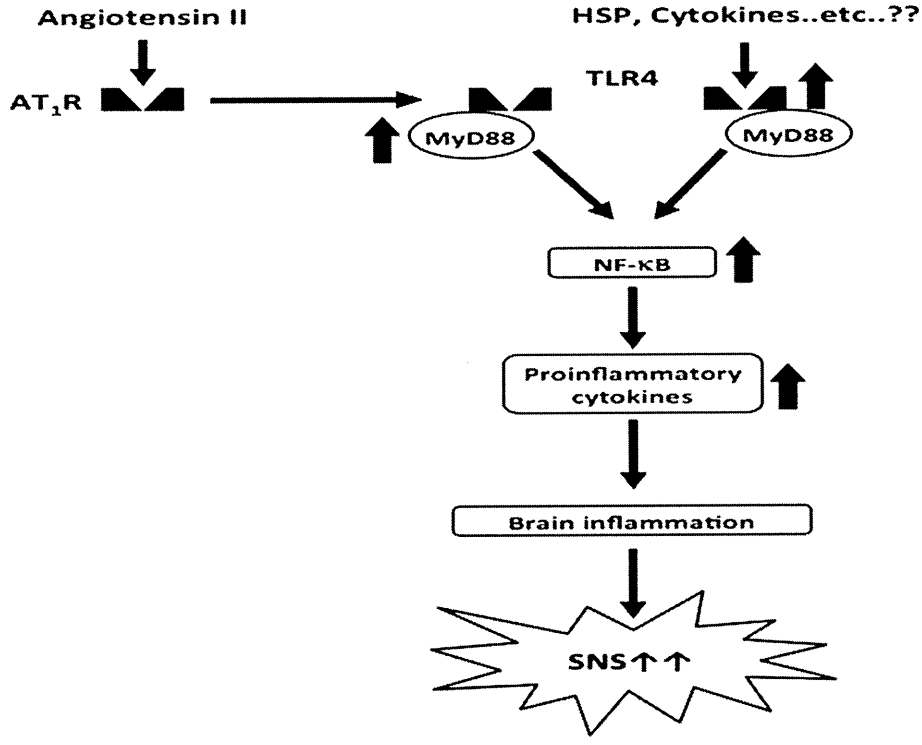

FIGURE 7. The scheme showing the cascade suggested by the results of the present study.

that activation of the AT_1R in those nuclei deteriorates the cardiac remodeling process through the TLR4 and MyD88 signaling. We suppressed the AT_1R–TLR4 pathway by the ICV infusion of the AT_1R blocker only for 14 days, and the activity of the SNS might be inhibited only for several days. We consider that the improvement of the LV function might need for longer period, at least for several months.

A previous report suggested that the ICV infusion of lipopolysaccharide (LPS), an agonist of the TLR4, elicits the activation of the SNS via proinflammatory cytokines and that the LPS increases the expression level of the AT_1R, NAD(P)H oxidase activity, and MAPK activity.[17] Other studies indicate that the blockade of the AT_1R decreases the expression level of the TLR4 in mesangial and smooth muscle cells.[31–34] In addition, we previously demonstrated that the AT_1R–NAD(P)H oxidase–MAPK pathway in the brainstem activates the SNS.[18] In the present study, we demonstrated that the ICV infusion of the AT_1R blocker inhibits the expression levels of the TLR4, MyD88, and NF-κB with sympathoinhibition and that the ICV infusion of the exogenous angiotensin II increases the expression level of the MyD88 with sympathoexcitation. Together with these previous and our findings, we consider that the upstream of the inflammation mediated by the TLR4 and MyD88 in the brain might be the AT_1R.

STUDY LIMITATIONS

There are some limitations in the present study. First, we did not show the direct evidence that the suppression of the AT_1R or TLR4 only in the brain reduced the enhanced central sympathetic outflow in the MI-induced HF because no agents for pharmacological inhibition of the TLR4 are available. Actually, there are already several studies of the MI-induced HF in the systemic *TLR4* gene knockout mice.[42,43] To gain a better understanding of the AT_1R-mediated TLR4 activation related to sympathoexcitation in MI-induced HF, future experiments using the genetically *TLR4* knockout mice will be needed. Second, we did not determine the ligand of the TLR4 in the present study. It has been suggested that not only LPS but also heat-shock protein or matrix components, such as fibronectin, hyaluronic acid, and fragments of heparan sulfate, have been reported to activate the TLR4[44] and that heat-shock protein 60 was in plasma after the ligation of LCA.[45] Further studies are necessary to examine the endogenous ligands of the TLR4 in the brain of the MI-induced HF mice.

CONCLUSIONS

In conclusion, our findings suggest that activation of the AT_1R in the brainstem enhances the central sympathetic outflow through at least in part the inflammation mediated by the TLR4 and MyD88 in mice with MI-induced HF (Fig. 7).

ACKNOWLEDGMENTS

This study was supported by a Grant-in-Aid for Scientific Research from the Japan Society for the Promotion of Science (B193290231, 33790709, and S23220013), and, in part, a Kimura Memorial Foundation Research Grant.

REFERENCES

1. Meredith IT, Eisenhofer G, Lambert GW, et al. Cardiac sympathetic nervous activity in congestive heart failure. Evidence for increased neuronal norepinephrine release and preserved neuronal uptake. *Circulation*. 1993;88:136–145.
2. Francis GS. The relationship of the sympathetic nervous system and the renin-angiotensin system in congestive heart failure. *Am Heart J*. 1989; 118:642–648.
3. Packer M. The neurohormonal hypothesis: a theory to explain the mechanism of disease progression in heart failure. *J Am Coll Cardiol*. 1992; 20:248–254.
4. Eichhorn EJ, Bristow MR. Medical therapy can improve the biological properties of the chronically failing heart. A new era in the treatment of heart failure. *Circulation*. 1996;94:2285–2296.
5. Goldsmith SR. Angiotensin II and sympathoactivation in heart failure. *J Cardiac Fail*. 1999;5:139–145.
6. Liu JL, Zucker IH. Regulation of sympathetic nerve activity in heart failure: a role for nitric oxide and angiotensin II. *Circ Res*. 1999;84:417–423.
7. Gao L, Wang W, Li YL, et al. Superoxide mediates sympathoexcitation in heart failure: roles of angiotensin II and NAD(P)H oxidase. *Circ Res*. 2004;95:937–944.
8. Murakami H, Liu JL, Zucker IH. Angiotensin II blockade [corrected] enhances baroreflex control of sympathetic outflow in heart failure. *Hypertension*. 1997;29:564–569.
9. Lindley TE, Doobay MF, Sharma RV, et al. Superoxide is involved in the central nervous system activation and sympathoexcitation of myocardial infarction-induced heart failure. *Circ Res*. 2004;94:402–409.
10. Liu D, Gao L, Roy SK, et al. Neuronal angiotensin II type 1 receptor upregulation in heart failure: activation of activator protein 1 and Jun N-terminal kinase. *Circ Res*. 2006;99:1004–1011.
11. Ahmad M, White R, Tan J, et al. Angiotensin-converting enzyme inhibitors, inhibition of brain and peripheral angiotensin-converting enzymes, and left ventricular dysfunction in rats after myocardial infarction. *J Cardiovasc Pharmacol*. 2008;51:565–572.
12. Zucker IH, Schultz HD, Patel KP, et al. Regulation of central angiotensin type 1 receptors and sympathetic outflow in heart failure. *Am J Physiol Heart Circ Physiol*. 2009;297:H1557–H1566.
13. Kimura Y, Hirooka Y, Kishi T, et al. Role of inducible nitric oxide synthase in rostral ventrolateral medulla in blood pressure regulation in spontaneously hypertensive rats. *Clin Exp Hypertens*. 2009;31:281–286.
14. Yu Y, Zhang ZH, Wei SG, et al. Brain perivascular macrophages and the sympathetic response to inflammation in rats after myocardial infarction. *Hypertension*. 2010;55:652–659.
15. Marvar PJ, Thabet SR, Guzik TJ, et al. Central and peripheral mechanisms of T-lymphocyte activation and vascular inflammation produced by angiotensin II-induced hypertension. *Circ Res*. 2010;107:263–270.
16. Kimura Y, Hirooka Y, Sagara Y, et al. Overexpression of inducible nitric oxide synthase in rostral ventrolateral medulla causes hypertension and sympathoexcitation via an increase in oxidative stress. *Circ Res*. 2005;96: 252–260.
17. Zhang ZH, Yu Y, Wei SG, et al. Centrally administered lipopolysaccharide elicits sympathetic excitation via NAD(P)H oxidase-dependent mitogen-activated protein kinase signaling. *J Hypertens*. 2010;28:806–816.
18. Kishi T, Hirooka Y, Konno S, et al. Angiotensin II type 1 receptor-activated caspase-3 through ras/mitogen-activated protein kinase/extracellular signal-regulated kinase in the rostral ventrolateral medulla is involved in sympathoexcitation in stroke-prone spontaneously hypertensive rats. *Hypertension*. 2010;55:291–297.
19. Akira S, Takeda K. Toll-like receptor signalling. *Nat Rev*. 2004;4: 499–511.
20. Caso JR, Pradillo JM, Hurtado O, et al. Toll-like receptor 4 is involved in brain damage and inflammation after experimental stroke. *Circulation*. 2007;115:1599–1608.
21. Alfonso-Loeches S, Pascual-Lucas M, Blanco AM, et al. Pivotal role of TLR4 receptors in alcohol-induced neuroinflammation and brain damage. *J Neurosci*. 2010;30:8285–8295.
22. Gorina R, Font-Nieves M, Marquez-Kisinousky L, et al. Astrocyte TLR4 activation induces a proinflammatory environment through the interplay between MyD88-dependent NFkB signaling, MAPK, and Jak1/Stat1 pathways. *Glia*. 2011;59:242–255.
23. Lehnardt S, Massillon L, Follett P, et al. Activation of innate immunity in the CNS triggers neurodegeneration through a toll-like receptor 4-dependent pathway. *Proc Natl Acad Sci U S A*. 2003;100:8514–8519.
24. Wolf G, Bohlender J, Bondeva T, et al. Angiotensin II upregulates toll-like receptor 4 on mesangial cells. *J Am Soc Nephrol*. 2006;17: 1585–1593.
25. Wu J, Yang X, Zhang YF, et al. Angiotensin II upregulates toll-like receptor 4 and enhances lipopolysaccharide-induced CD40 expression in rat peritoneal mesothelial cells. *Inflamm Res*. 2009;58:473–482.
26. Lazartigues E, Sinnayah P, Augoyard G, et al. Enhanced water and salt intake in transgenic mice with brain-restricted overexpression of angiotensin (AT1) receptors. *Am J Physiol*. 2008;295:R1539–R1545.
27. Kishi T, Hirooka Y, Sakai K, et al. Overexpression of eNOS in the RVLM causes hypotension and bradycardia via GABA release. *Hypertension*. 2001;38:896–901.
28. Kishi T, Hirooka Y, Ito K, et al. Cardiovascular effects of overexpression of endothelial nitric oxide synthase in the rostral ventrolateral medulla in stroke-prone spontaneously hypertensive rats. *Hypertension*. 2002;39: 264–268.
29. Kishi T, Hirooka Y, Kimura Y, et al. Increased reactive oxygen species in rostral ventrolateral medulla contribute to neural mechanisms of hypertension in stroke-prone spontaneously hypertensive rats. *Circulation*. 2004;109:3257–3262.
30. Zimmerman MC, Lazartigues E, Sharma RV, et al. Hypertension caused by angiotensin II infusion involves increased superoxide production in the central nervous system. *Circ Res*. 2004;95:210–216.
31. Yang J, Jiang H, Yang J, et al. Valsartan preconditioning protects against myocardial ischemia-reperfusion injury through TLR4/NF-kB signaling pathway. *Mol Cell Biochem*. 2009;330:39–46.
32. Dasu MR, Riosvelasco AC, Jialal I. Candesartan inhibits toll-like receptor expression and activity both in vitro and in vivo. *Atherosclerosis*. 2009;202:76–83.
33. Lv J, Jia R, Yang D, et al. Candesartan attenuates angiotensin II-induced mesangial cell apoptosis via TLR4/MyD88 pathway. *Biochem Biophys Res Commun*. 2009;380:81–86.
34. Cheng XW, Song H, Sasaki T, et al. Angiotensin type 1 receptor blocker reduces intimal neovascularization and plaque growth in apolipoprotein E-deficient mice. *Hypertension*. 2011;57:981–989.
35. Hirooka Y, Kishi T, Sakai K, et al. Imbalance of central nitric oxide and reactive oxygen species in the regulation of sympathetic activity and neural mechanisms of hypertension. *Am J Physiol*. 2011;300: R818–R826.
36. Van Tassell BW, Seropian IM, Toldo S, et al. Pharmacologic inhibition of myeloid differentiation factor 88 (MyD88) prevents left ventricular dilation and hypertrophy after experimental acute myocardial infarction in the mouse. *J Cardiovasc Pharmacol*. 2010;55:385–390.
37. Dampney RAL. Functional organization of central pathways regulating the cardiovascular system. *Physiol Rev*. 1994;74:323–364.
38. Guyenet PG. The sympathetic control of blood pressure. *Nat Rev Neurosci*. 2006;7:335–346.
39. McKinley MJ, Albinson AL, Allen AM, et al. The brain renin-angiotensin system: location and physiological roles. *Int J Biochem Cell Biol*. 2003;35: 901–918.
40. Dupont AG, Brouwers S. Brain angiotensin peptides regulate sympathetic tone and blood pressure. *J Hypertens*. 2010;28:1599–1610.
41. Allen AM, O'Callaghan EL, Chen D, et al. Central neural regulation of cardiovascular function by angiotensin: a focus on the rostral ventrolateral medulla. *Neuroendocrinology*. 2009;89:361–369.
42. Wang E, Feng Y, Zhang M, et al. Toll-like receptor 4 signaling confers cardiac protection against ischemic injury via inducible nitric oxide synthase- and soluble guanylate cyclase-dependent mechanisms. *Anesthesiology*. 2011;114:603–613.
43. Riad A, Jäger S, Sobirey M, et al. Toll-like receptor-4 modulates survival by induction of left ventricular remodeling after myocardial infarction in mice. *J Immunol*. 2008;180:6954–6961.
44. Takeda K, Kaisho T, Akira S. Toll-like receptors. *Annu Rev Immunol*. 2003;21:335–376.
45. Lin L, Kim SC, Wang Y, et al. HSP60 in heart failure: abnormal distribution and role in cardiac myocyte apoptosis. *Am J Physiol*. 2007;293: H2238–H2247.

Neuregulin-1/ErbB signaling in rostral ventrolateral medulla is involved in blood pressure regulation as an antihypertensive system

Ryuichi Matsukawa[a], Yoshitaka Hirooka[b], Masaaki Nishihara[a], Koji Ito[a] and Kenji Sunagawa[a]

Objectives **Neuregulin-1 (NRG-1), located in the central nervous system (CNS), plays an important role in synaptic function, neurite outgrowth, and survival of neurons and glia acting on the ErbB receptor family. However, the functional role of NRG-1/ErbB signaling in the CNS and blood pressure regulation is unknown, particularly in the rostral ventrolateral medulla (RVLM), a major vasomotor center. Thus, we investigated whether NRG-1/ErbB signaling in the RVLM is involved in blood pressure regulation.**

Methods and results **Microinjection of NRG-1 into the RVLM decreased arterial blood pressure, heart rate (HR), and renal sympathetic nerve activity (RSNA) in Wistar rats. In contrast, microinjection of an ErbB2 or ErbB4 inhibitor into the RVLM increased arterial pressure, HR, and RSNA. ErbB2 expression levels in the brainstem were significantly lower in spontaneously hypertensive rats (SHRs) than in Wistar–Kyoto (WKY) rats. Depressor responses to NRG-1 and pressor responses to the ErbB2 inhibitor were significantly smaller in SHRs than in WKY rats ($P<0.05$). Furthermore, the inhibition of ErbB2 expression in the RVLM by RNA interference significantly increased arterial pressure, HR, and urinary norepinephrine excretion in conscious WKY rats ($P<0.01$).**

Conclusion **Our findings indicate that the NRG-1/ErbB signaling in the RVLM has depressor and sympathoinhibitory effects. Reduced NRG/ErbB2 signaling in the RVLM may contribute to the neural mechanisms of hypertension.** *J Hypertens* **29:1735–1742 © 2011 Wolters Kluwer Health | Lippincott Williams & Wilkins.**

Journal of Hypertension 2011, **29**:1735–1742

Keywords: blood pressure, ErbB, hypertension, neuregulin-1, rostral ventrolateral medulla, sympathetic nervous system

Abbreviations: CNS, central nervous system; GABA, γ-aminobutyric acid; HR, heart rate; MAP, mean arterial pressure; NRG-1, neuregulin-1; RSNA, renal sympathetic nerve activity; RVLM, rostral ventrolateral medulla; SHR, spontaneous hypertensive rat; siRNA, small-interference RNA; uNE, urinary norepinephrine excretion; WKY, Wistar–Kyoto

[a]Department of Cardiovascular Medicine and [b]Department of Advanced Cardiovascular Regulation and Therapeutics, Kyushu University Graduate School of Medical Sciences, Fukuoka, Japan

Correspondence to Yoshitaka Hirooka, MD, PhD, FAHA, Department of Advanced Cardiovascular Regulation and Therapeutics, Kyushu University Graduate School of Medical Sciences, 3–1–1 Maidashi, Higashi-ku, Fukuoka 812–8582, Japan
Tel: +81 92 6425356; fax: +81 92 6425374;
e-mail: hyoshi@cardiol.med.kyushu-u.ac.jp

Received 23 March 2011 **Revised** 23 May 2011
Accepted 25 May 2011

Introduction

Neuregulin-1 (NRG-1) is a member of the epidermal growth factor family, which is involved in cell–cell communication [1,2]. NRG-1 is expressed in the nervous system, heart, and other organ systems [1–3]. NRG-1 binds to the extracellular domain of the tyrosine kinase ErbB3 or ErbB4, which often leads to the formation of ErbB heterodimers with ErbB2. This activates intracellular signaling pathways leading to synaptic function, neurite outgrowth, and survival of neurons and glia [3–5]. It is also known that NRG-1 and ErbB receptors are widely distributed in the central nervous system (CNS), including the brainstem [6–10]. Several studies have demonstrated the involvement of NRG-1/ErbB signaling in the regulation of neurotransmitters, such as L-glutamate and γ-aminobutyric acid (GABA) [11,12]. In addition, ErbB2 is known to be involved in the development of glial cells and their transformation into astrocytes [13]. However, little is known regarding the role of the NRG-1/ErbB signaling pathway in the brainstem and the action of this pathway on blood pressure regulation.

With regard to CNS blood pressure regulation, the rostral ventrolateral medulla (RVLM) of the brainstem is one of the most important regions involved in central cardiovascular regulation [14–17]. RVLM neurons project toward sympathetic preganglionic neurons in the intermediolateral cell column of the spinal cord and provide an essential excitatory drive, thereby maintaining sympathetic vasomotor tone [14]. In addition, the RVLM neurons regulate sympathetic vasomotor tone by integrating the inputs from baroreceptors, chemoreceptors, and higher autonomic nuclei [18]. Accumulating evidence suggests that increased RVLM activity leads to chronic sympathetic hyperactivity in many forms of hypertension [17]. For example, in spontaneously hypertensive rats (SHRs), excitation of the RVLM vasomotor

0263-6352 © 2011 Wolters Kluwer Health | Lippincott Williams & Wilkins DOI:10.1097/HJH.0b013e32834937d6

neurons is increased by L-glutamate-mediated excitation and decreased GABA-mediated inhibition [16,17]. Therefore, the aim of the present study was to determine whether NRG-1/ErbB signaling in the RVLM contributes to blood pressure regulation through the sympathetic nervous system, and, if so, whether alteration of this signaling in the RVLM occurs in SHRs, leading to the activation of the sympathetic nervous system associated with neurogenic hypertensive mechanisms. We investigated the effect of NRG-1 and the ErbB receptor blockers injected into the RVLM on arterial blood pressure, heart rate (HR), and sympathetic nervous system activity. Expression levels of NRG-1 and ErbB receptors were also evaluated. These effects were examined in SHRs to elucidate the role of this signaling in hypertension. Finally, we further examined the effects of this signaling in conscious rats using small-interference RNA (siRNA) techniques.

Methods

This study was reviewed and approved by the Committee on Ethics of Animal Experiments, Kyushu University Graduate School of Medical Sciences, and it was performed according to the Guidelines for Animal Experiments of Kyushu University.

Microinjection studies

Animals were anesthetized and measured for arterial pressure, HR and renal sympathetic nerve activity (RSNA). For details of general surgical preparation, see online Data Supplemental Digital Content 1, http://links.lww.com/HJH/A108. Microinjections into the RVLM were made according to the following protocols: unilateral microinjection of recombinant NRG-1β (NRG-1β: 0.025, 0.25, and 2.5 pmol in 50 nl injections; Ray Biotech, Norcross, Georgia, USA) in Wistar rats and NRG-1β (2.5 pmol in 50 nl injections) was microinjected in Wistar–Kyoto (WKY) rats and SHRs; bilateral microinjections of the ErbB2 antagonists AG825 (0.5 pmol in 50 nl injections; Santa Cruz Biotechnology, Santa Cruz, California, USA) in Wistar rats, WKY rats, and SHRs; bilateral microinjections of the ErbB4 antagonists AG1478 (0.5 pmol in 50 nl injections; Santa Cruz Biotechnology) in Wistar rats, WKY rats, and SHRs; unilateral microinjection of NRG-1β (2.5 pmol in 50 nl injections) 10 min after unilateral injection of both AG825 (0.5 pmol in 50 nl injections) and AG1478 (0.5 pmol in 50 nl injections) in Wistar rats; unilateral microinjection of NRG-1β (2.5 pmol in 50 nl injections) 5 min after unilateral injection of the GABA-A receptor antagonist bicuculline (100 pmol in 50 nl injections; Santa Cruz) in Wistar rats; and unilateral microinjection of L-glutamate (1.0 nmol in 50 nl injections; Nakarai Tesque, Fukuoka, Japan) 10 min after unilateral injection of NRG-1β (2.5 pmol in 50 nl injections) in Wistar rats. Arterial pressure, HR, and RSNA are monitored in the first (2.5 pmol NRG-1β), second, and third protocol. Arterial pressure and HR are monitored in the first (0.025 and 0.25 pmol NRG-1β) and the fourth to sixth protocol. Dosages of reagents were determined as follows. The dose of NRG-1β was determined on the basis of previous studies [19,20]. Additionally, we confirmed the dose response in the present study. Doses of AG825 and AG1478 were determined on the basis of previous studies and half maximal inhibitory concentration (IC_{50}) values [21–25]. Furthermore, to exclude the peripheral effects of the agents, we performed intravenous administration of the agents (the same amount of the agents used in microinjection studies in 0.2 ml isotonic saline). However, there were no effects on mean arterial pressure (MAP) and HR [ΔMAP: NRG-1 (2.5 pmol), -0.9 ± 1.8 mmHg; AG825 (1.0 pmol), 0.6 ± 1.8 mmHg; AG1478 (1.0 pmol), 0.3 ± 1.1 mmHg; and ΔHR: NRG-1, 0.6 ± 2.3 beats/min; AG825, 0.9 ± 2.8 beats/min; AG1478, 1.0 ± 0.9 beats/min ($n = 3$ for each)]. Doses of bicuculline and L-glutamate were determined on the basis of previous studies [26–28].

Western blot analysis

Western blots were made according to the following protocols: first, expressions of NRG-1 and ErbB receptors (ErbB2, ErbB3, and ErbB4) in the brainstem of 4-week-old and 12-week-old WKY rats and SHRs were confirmed. Rabbit IgG monoclonal antibodies against NRG-1 (1 : 1000), ErbB2 (1 : 1000), ErbB3 (1 : 1000), and ErbB4 (1 : 1000) were used as the primary antibody. Additionally, expression of ErbB2 in the cerebral cortex or hypothalamus of 12-week-old WKY rats and SHRs was confirmed. Second, in a study of chronic inhibition of ErbB2 in the RVLM by siRNA, western blot was performed to confirm the effects of RNA interference on the ErbB2 receptor using RVLM tissues of WKY rats. At 0, 1, 5, and 14 days after administration of ErbB2 or control siRNA (siErbB2 or siControl), rats were anesthetized using sodium pentobarbital and perfused transcardially with PBS. RVLM tissues defined according to a rat brain atlas were obtained as previously described [29]. Anti-ErbB2 antibody (1 : 1000) was used. For details see online Data Supplemental Digital Content 1, http://links.lww.com/HJH/A108.

In-vivo small-interference RNA technique

The siErbB2 sequence was determined as described in a previous study [30]. Specific siErbB2 (AAGUGUGUG UACCGGCACAGACA) and scrambled siRNA (siControl: AGCCUAACUGAACGCGUAGGA), as a control, were purchased from Koken, Tokyo, Japan. Furthermore, we used the in-vivo siRNA delivery kit AteloGene (Koken) for stable local delivery of the siRNA into the RVLM. SiErbB2 or siControl was administered into the RVLM, and MAP and HR were monitored using radiotelemetry system for 14 days. For details see online Data Supplemental Digital Content 1, http://links.lww.com/HJH/A108.

Measurement of urinary norepinephrine excretion

We measured urinary norepinephrine excretion (uNE) concentration before and at 1, 7, and 14 days after the start of the administration of siRNA and calculated uNE as described previously [26,31].

Statistical analysis

All values are expressed as the mean ± SEM. Differences were considered significant when the P value was less than 0.05. For details see online Data Supplemental Digital Content 1, http://links.lww.com/HJH/A108.

Results

Baseline mean arterial pressure and heart rate of microinjection study

The baseline MAP and HR in microinjection protocols of NRG-1β, AG825, and AG1478 are described in Supplemental Digital Content 2, Online Table 1, http://links.lww.com/HJH/A109.

Effects of neuregulin-1 injection into the rostral ventrolateral medulla on arterial blood pressure, heart rate, and renal sympathetic nerve activity

Microinjection of NRG-1β (2.5 pmol) into the RVLM unilaterally significantly decreased MAP, HR, and RSNA [ΔMAP, −22.3 ± 1.8 mmHg; ΔHR, −36.1 ± 5.5 beats/min; ΔRSNA %baseline, −36.9 ± 6.2%; $P < 0.01$, $n = 5$; Fig. 1a]. These changes occurred slowly and peaked approximately 10–15 min after injection. The depressor and bradycardic responses induced by NRG-1β occurred in a dose-dependent manner (Fig. 1b).

Fig. 1

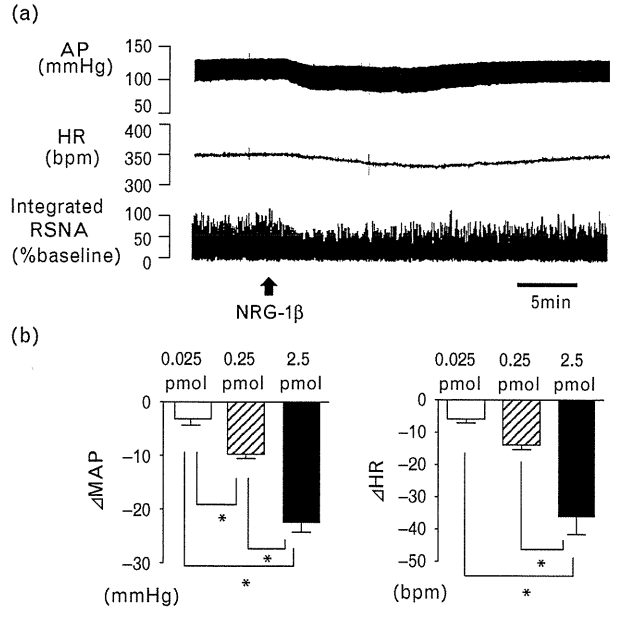

Response of arterial pressure (AP), heart rate (HR), and renal sympathetic nerve activity (RSNA) to unilateral microinjection of neuregulin-1β (NRG-1β) into the rostral ventrolateral medulla of Wistar rats. (a) Raw data of changes in AP, HR, and RSNA in response to microinjection of NRG-1β (2.5 pmol). (b) Group data of changes in mean AP (MAP) and HR in response to microinjection of NRG-1β. Values are expressed as mean ± SEM. *$P < 0.05$ ($n = 5$ per injection).

Effects of inhibition of ErbB2 and ErbB4 receptors in the rostral ventrolateral medulla on mean arterial pressure, heart rate, and renal sympathetic nerve activity

MAP, HR, and RSNA values increased significantly after bilateral injection of the ErbB2 receptor blocker, AG825 (1.0 pmol), into the RVLM (ΔMAP, +17.6 ± 2.3 mmHg; ΔHR, +16.5 ± 1.1 beats/min; ΔRSNA %baseline, +29.6 ± 4.1%; $P < 0.01$, $n = 5$; Fig. 2a, c). These variables also increased after injection of the ErbB4 inhibitor, AG1478 (1.0 pmol) (ΔMAP, 11.0 ± 1.6 mmHg; ΔHR, 12.9 ± 1.9 beats/min; ΔRSNA %baseline, +18.3 ± 3.8%; $P < 0.01$, $n = 5$; Fig. 2b, c). These changes occurred slowly and peaked approximately 10–15 min after microinjection of the blockers. After microinjection of both AG825 (0.5 pmol) and AG1478 (0.5 pmol), the depressor response to NRG-1β (2.5 pmol) injected into the RVLM was nearly abolished (ΔMAP, −22.3 ± 1.8 vs. −2.0 ± 0.7 mmHg; ΔHR, −36.1 ± 5.5 vs. −2.5 ± 0.7 beats/min; $P < 0.01$, $n = 5$ for each; Fig. 2d).

Furthermore, to demonstrate that the effects of the reagents in the RVLM are site specific, microinjections of NRG-1β and AG825 were performed 1.0-mm dorsal apart from the RVLM in Wistar rats. The changes in MAP, HR, and RSNA were not significant (Supplemental Digital Content 2, Online Table 2, http://links.lww.com/HJH/A109).

Effect of blockade of γ-aminobutyric acid-A receptors in the rostral ventrolateral medulla on the depressor response to neuregulin-1

The baseline MAP before NRG-1β injection increased after the injection of the GABA-A receptor antagonist bicuculline (100 pmol) (MAP increased from 118.3 ± 3.8 to 146.3 ± 10.7 mmHg, whereas HR decreased from 337.8 ± 13.2 to 332.3 ± 17.6 beats/min). The depressor response to NRG-1β (2.5 pmol) into the RVLM was significantly attenuated after bicuculline injection (ΔMAP, −22.9 ± 2.9 vs. −4.6 ± 2.0 mmHg; ΔHR, −38.1 ± 5.5 vs. −11.9 ± 2.3 beats/min; $P < 0.01$, $n = 5$ for each).

Effect of neuregulin-1 in the rostral ventrolateral medulla on the pressor response to L-glutamate

The baseline MAP before L-glutamate injection decreased after NRG-1β injection (2.5 pmol) from 126.0 ± 5.2 to 109.9 ± 4.3 mmHg. The pressor response to L-glutamate (1.0 nmol) into the RVLM was significantly attenuated after NRG-1β injection (ΔMAP, 23.4 ± 1.0 vs. 10.8 ± 1.6 mmHg; $P < 0.01$, $n = 5$ for each).

ErbB receptors expression levels in the brainstem in Wistar–Kyoto and spontaneously hypertensive rats

NRG-1 and ErbB receptors (ErbB2, ErbB3, and ErbB4) are expressed in the brainstem in both the 12-week-old

Fig. 2

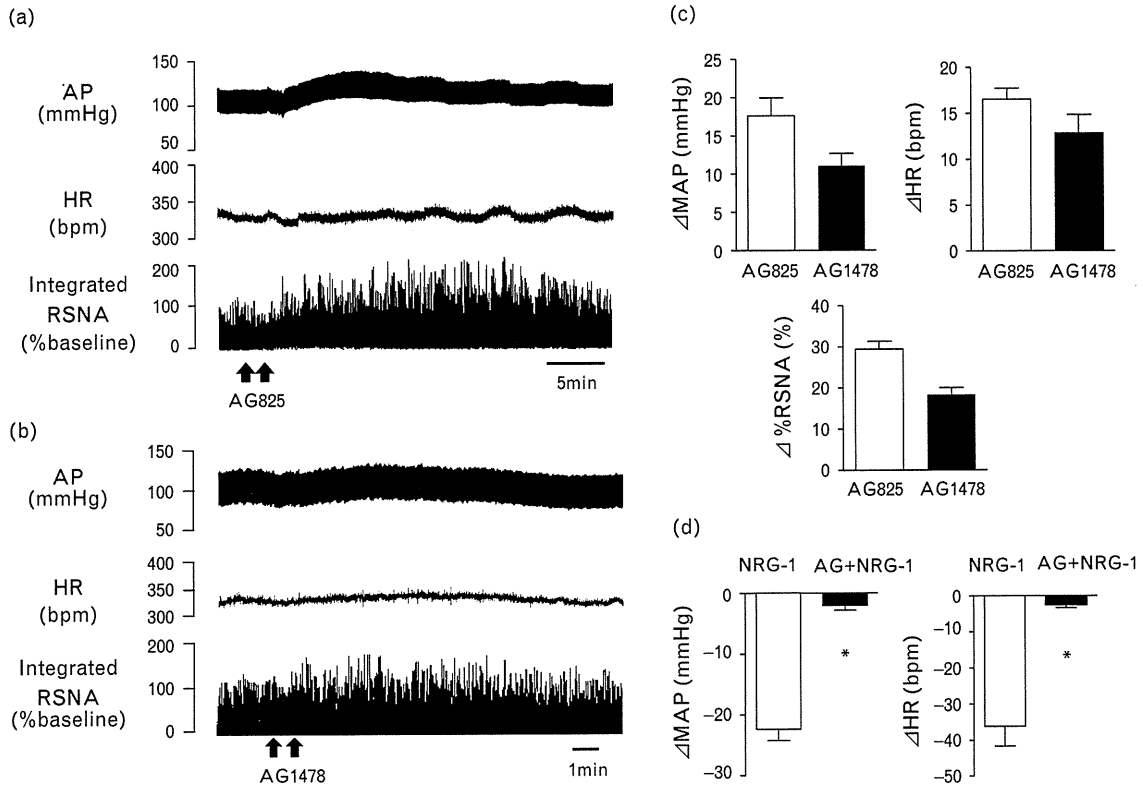

Response of arterial pressure (AP), heart rate (HR), and renal sympathetic nerve activity (RSNA) to bilateral microinjection of the ErbB2 antagonist (AG825) and ErbB4 antagonist (AG1478) into the rostral ventrolateral medulla (RVLM) of Wistar rats. (a) Raw data of changes in AP, HR, and RSNA response to microinjection of AG825 (1.0 pmol). (b) Raw data of changes in AP, HR, and RSNA response to microinjection of AG1478 (1.0 pmol). (c) Group data of changes in mean AP (MAP), HR, and RSNA in response to microinjection of AG825 or AG1478. Values are expressed mean ± SEM ($n = 5$ per injection). (d) Effect of blockade of both ErbB2 and ErbB4 receptors in the RVLM on the depressor response to NRG-1β. NRG-1 represents unilateral microinjection of neuregulin-1β (NRG-1β, 2.5 pmol) without pretreatment into the RVLM of Wistar rats and AG+NRG-1 represents unilateral microinjection of NRG-1β (2.5 pmol) with prior injection of both AG825 (0.5 pmol) and AG1478 (0.5 pmol) into the RVLM of Wistar rats. Values are expressed as mean ± SEM. *$P < 0.05$ ($n = 5$ for each).

SHRs and WKY rats. However, only ErbB2 expression levels were significantly lower in SHRs than in WKY rats ($P < 0.05$, $n = 5$ for each; Fig. 3a). We further examined NRG-1 and ErbB receptor expression levels in the brainstem of 4-week-old prehypertensive SHRs and age-matched WKY rats. ErbB2 expression levels were significantly lower in 4-week-old SHRs than in WKY rats ($n = 5$ for each; Fig. 3a). NRG-1 and other ErbB receptor expression levels, however, were similar between SHRs and WKY rats for both ages ($n = 5$ for each; Fig. 3b). On the contrary, in cerebral cortex and hypothalamus, ErbB2 expression levels were similar between 12-week-old SHRs and WKY rats (Fig. 3c).

Acute effects of neuregulin-1 or ErbB inhibitors on mean arterial pressure in Wistar–Kyoto and spontaneously hypertensive rats

The magnitudes of decreases in MAP, HR, and RSNA evoked by the unilateral injection of NRG-1β (2.5 pmol) into the RVLM were significantly smaller in SHRs than in WKY rats (ΔMAP, −23.3 ± 2.5 vs. −12.5 ± 1.7 mmHg, $P < 0.01$; ΔHR, −29.9 ± 4.0 vs. −15.5 ± 1.6 beats/min, $P < 0.05$; ΔRSNA %baseline, −33.8 ± 4.2 vs. −17.2 ± 3.0%, $P < 0.01$; $n = 5$ for each; Fig. 4a). The magnitudes of increases in MAP, HR, and RSNA evoked by the injection of AG825 (1.0 pmol) were significantly smaller in SHRs than in WKY rats (ΔMAP, +16.7 ± 1.4 vs. +8.9 ± 1.0 mmHg, $P < 0.05$; ΔHR, +20.5 ± 4.2 vs. +10.0 ± 1.2 beats/min, $P < 0.05$; ΔRSNA %baseline, +31.8 ± 4.9 vs. +17.8 ± 2.3%, $P < 0.01$; $n = 5$ for each; Fig. 4b). In contrast, the magnitudes of increase in MAP, HR, and RSNA evoked by the injection of AG1478 (1.0 pmol) did not differ between SHRs and WKY rats (ΔMAP, +8.7 ± 0.9 vs. +9.9 ± 1.2 mmHg; ΔHR, +11.2 ± 1.8 vs. +10.9 ± 0.8 beats/min; ΔRSNA %baseline, +18.9 ± 3.5 vs. +19.8 ± 3.7%; P = NS, $n = 5$; Fig. 4c).

Effects of local inhibition of ErbB2 in the rostral ventrolateral medulla caused by in-vivo small-interference RNA on mean arterial pressure, heart rate, and urinary norepinephrine excretion in conscious Wistar–Kyoto rats

Inhibition of ErbB2 receptors in the RVLM using siRNA increased MAP and HR between days 1 and 5

Fig. 3

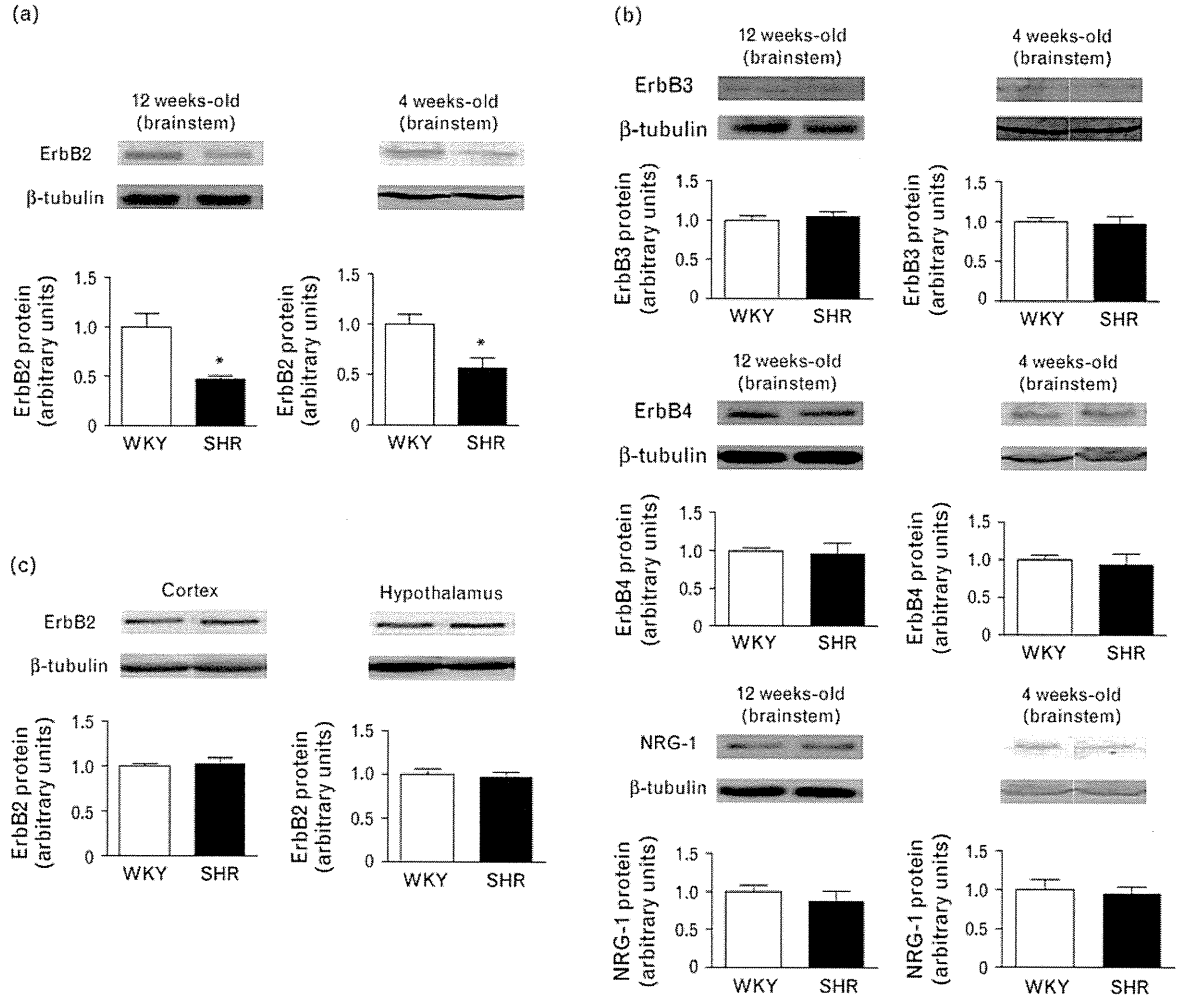

Western blot of (a) ErbB2, (b) neuregulin-1 (NRG-1), ErbB3, and ErbB4 in the brainstem of 12-week-old and 4-week-old Wistar–Kyoto (WKY) rats and spontaneously hypertensive rats (SHRs). (c) Western blot of ErbB2 in cerebral cortex and hypothalamus of 12-week-old WKY rats and SHRs. The densitometric average was normalized to the values obtained from the analysis of β-tubulin as internal control. Expressions are shown relative to that in WKY rats, which were assigned a value of 1. Values are expressed as mean ± SEM. $^*P < 0.05$ (vs. WKY rats, $n = 5$ for each).

after the siErbB2 treatment in WKY rats. In contrast, these variables did not change in the siControl-treated rats ($P < 0.05$, $n = 5$ for each; Fig. 5a). Twenty-four-hour uNE levels at day 1 and 7 were significantly greater in siErbB2 than that in siControl-treated rats ($P < 0.01$, $n = 5$ for each; Fig. 5b). The ErbB2 protein expression levels of RVLM in siErbB2-treated rats were successfully inhibited between days 1 and 5 compared with day 0 (Fig. 5c).

Discussion

The findings of the present study are the first to suggest that NGR-1/ErbB signaling in the RVLM reduces blood pressure through the inhibition of the sympathetic nervous system activity. This suggestion is supported by the results of microinjection of NRG-1 or ErbB2 and ErbB4 antagonists into the RVLM, which demonstrated a decrease or increase in blood pressure associated with changes in RSNA in acute anesthetized rats. This is further supported by the experiments involving the inhibition of ErbB2 receptors in the RVLM using siRNA for ErbB2 receptors in chronic conscious state. Furthermore, our findings suggest that signaling in the RVLM is impaired in SHRs. This is based on the results indicating that the depressor response to NRG-1 and pressor response to the ErbB2 in the RVLM are attenuated in SHRs together with the reduced ErbB2 expression levels in the RVLM of SHRs. Therefore, signaling abnormalities in the RVLM may contribute to, at least in part, the neurogenic mechanisms of hypertension.

NRG-1/ErbB signaling in the RVLM was found to have depressor effects with sympathoinhibition. Microinjection of recombinant NRG-1β into the RVLM decreased arterial pressure, HR, and RSNA in anesthetized normotensive rats. In contrast, microinjection of the ErbB2